Rybachuk, Maksym and Bell, John M. (2007) Synthesis of Diamond-Like Carbon Films Using a Bi-Modal Sputter Deposition with Xe IONS. *Surface Review and Letters (SRL)* 14(4):pp. 735-738.

SYNTHESIS OF DIAMOND-LIKE CARBON FILMS USING A BI-MODAL SPUTTER DEPOSITION WITH *Xe* IONS

MAKSYM RYBACHUK, JOHN M. BELL
Faculty of Built Environment and Engineering, Queensland University of Technology
Gardens Point, 2 George St., Brisbane Qld 4001, Australia

Received
Revised

An alternative approach to a sputtering process was examined where a single incident beam of *Xe* ions was used to simultaneously sputter a carbon target and bombard a growing film. There was a hypothesis that by positioning a substrate at grazing angles to the central axis of the ion beam, the additional energy provided would be beneficial to formation of sp^3 bonding. Amorphous carbon (*a-C*) and diamond-like carbon (DLC) films were synthesized by sputtering a graphite target from a Kaufmann-type ion source. Experimental results revealed that when a substrate was placed at grazing angles due to a secondary resputtering process, it was not possible to fabricate DLCs but only sp^2 rich polymeric *a-C*. For DLC synthesis the optimal angles of the target and the substrate to the ion flux were found to be 30º and 0º respectively and the ion energies of 0.8 – 1 keV.

1. Introduction

Sputtering is a common industrial process for fabrication of DLC and in a most common form the DC of RF sputtering of a graphite target electrode by *Ar* plasma is used. The term 'sputtering' is also applied to an ion beam sputtering where a beam of ions is used to sputter from a graphite target creating a carbon flux. Often an additional beam is used to bombard the growing film by delivering extra energy to densification process and promoting favorable morphological changes (Ref. 1). Using a single ion beam with a solid carbon source to synthesize amorphous carbon nitride in a reactive condition had been earlier reported by the Bell and co-workers (Ref. 2), where a graphite target was sputtered by using a nitrogen ion beam and a substrate was positioned parallel to the central axis of the beam.

In this work we examine a single ion beam deposition method and investigate whether a positioning of a substrate at low incident angles to the ion beam will result in beneficial structural changes (the increase of sp^3 fraction) of the growing DLC films.

2. Experimental Methods

2.1. Deposition Method

The sputter deposition was carried out on a CTP-700 high vacuum deposition system (Laserdyne Pty Ltd) fitted with a Kaufman-type ion source with a convex ion grids of 40 mm in diameter. Highly ordered pyrolytic graphite (HOPG) was used as the target and *Xe* gas was used as a feed gas to the ion gun. The geometry of the ion beam, sputtering target and substrate are illustrated in Fig. 1.

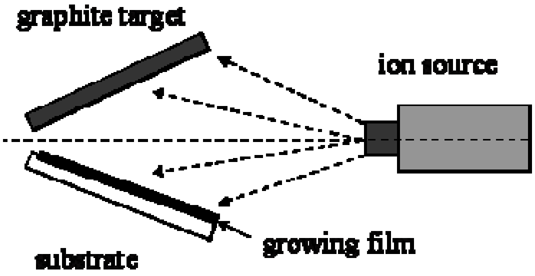

Fig. 1. Schematics of bi-modal ion beam sputter deposition, where a single ion beam is used for target sputtering and concurrent substrate bombardment.

Three values of the target - ion beam angle, α_t, were used: 15°; 30°; and 45°. The substrate to the ion beam flux angle, α_s was either 0° or 10°. The substrate was made of mild steel and was electrically connected with the target minimizing the surface charge accumulation during the deposition. The beam voltage was varied from 0.2 keV to 1.0 keV in 0.2 keV increments and carbon films were deposited onto *Si* <100> substrates. The operating parameters used during the deposition are summarized in Table 1.

Table 1. Operation variables for a bi-modal sputter deposition.

Base vacuum	2 x 10^{-5} Torr
Working pressure	4.1 - 4.2 x 10^{-4} Torr
Ion beam	0.2 - 1.0 keV at 10 mA
Accelerator	190 V at 1.0 mA
Discharge	60 V at 0.6 A
Filament	12.5-14.0 A
Neutralizer	2 mA, DC
Deposition time	30 ± 1 min

2.2. Characterization Methods

A Kimmon 5161R-GS Raman spectroscope with *He/Ca* laser at a wavelength of 325 nm was used to monitor individual sp^2 and sp^3 bonding in fabricated films. The power of the UV source was set below 1 mW to overcome sample damage during measurements and the sample was moved linearly at the speed of 10 µm/sec.

X-ray photoelectron spectroscopy (XPS), using a Kratos Ultra photoelectron spectroscope with a monochromated $Al\ K_\alpha$ 1486.6 eV X-ray source, was used to obtain C_{1s} spectra. The chamber vacuum level was maintained below 2 x 10^{-11} Torr. The spectrometer was calibrated by peak referencing of $Au\ 4f_{7/2}$ (BE of 84.0 eV) with respect to the Fermi level. Surface charging was not observed during the measurements. The C_{1s} scans were performed at pass energy of 20 eV with a resolution of 0.05 eV and dwell time was 250 msec.

Scanning Electron Microscopy using AEI Quanta 200 electron microscope was employed to examine frontal and cross sectional surfaces of the films. The films were found to display smooth and flat surfaces and thickness was found to vary from 0.1 (±0.01) to 10 (± 0.02) µm with thicker films corresponding to higher ion energy during the deposition.

3. Results and Discussion

Atomic scale Monte Carlo (MC) simulation for *Xe* ions interacting with a HOPG was performed using SRIM (Ref. 3) prior to experiments. The MC calculations indicated that optimal target angles, α_t for ion energies up to 1 keV were in the range of 15° to 30° giving an atom to ion yield of up to 29. In order to form DLC a metastable increase in density is required which causes the local bonding to change to sp^3 and the use of an infringing ion beam was aimed to achieve that. Table 2 shows the summary of the films types deposited under different *Xe* ion energies and at varying target and substrate to ion beam axis angles.

Table 2. Different film types synthesized at varying ion beam energies and target/substrate sputtering geometry. Note: “---" shows the absence of an observable film; “~” the experiment was not performed

Ion beam energy, keV	Target and substrate to the ion beam axis sputtering angles, α_t/α_s °					
	15/0	15/10	30/0	30/10	45/0	45/10
0.2	---	---	*SiC*	---	---	---
0.4	*SiC*	*SiC*	*a-C*	*SiC*	*SiC*	---
0.6	*a-C*	*SiC*	DLC	*a-C*	*a-C*	*SiC*
0.8	DLC	*SiC*	DLC	*a-C*	DLC	*SiC*
1.0	~	a-C	DLC	*a-C*	~	*a-C*

The results indicate that at α_s of 10° there was no carbon film formation at energies below 0.6 keV, that is for α_t/α_s of 30/10. At α_s of 10° and ion energy of 0.6 keV and above an interstitial layer of *SiC* was formed on the *Si* substrate providing the necessary nucleation sites for growth of *a-C* and DLC films. Whereas, when the substrate was parallel to the ion beam axis (α_s = 0°), the *a-C* film was formed at ion energies of 0.4 eV and above for α_t/α_s of 30/0. Fig. 2 shows a Raman spectrum of *a-C* films produced using the ion energy of 1.0 keV and at the target/substrate sputtering angles of α_t 30° and α_s 10°. It was unnecessarily to reconstitute the spectrum of Fig. 2 as the shape of the main carbon peak is characteristic of *a-C* films that are polymeric and essentially composed of sp^2 fraction. This is revealed by a dominating *D* band located approximately at 1350 –

1360 cm^{-1} corresponding to breathing vibrations of aromatic rings (Ref. 4).

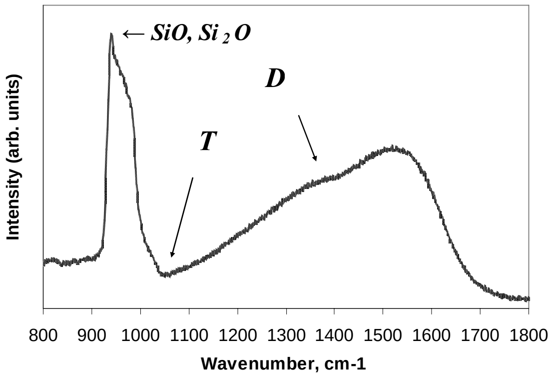

Fig 2. 325nm Raman spectra of *a-C* films fabricated at sputtering angles of α_t 30° and α_s 10° and ion energy of 1 keV.

The absence of T band at 1040 – 1090 cm^{-1} that corresponds to average vibrational density of states of sp^3 fraction (Ref. 4) is obvious; which means that there is no sp^3 bonding in synthesized *a-C* films. In addition, the presence of neighboring peaks at 930 – 980 cm^{-1} corresponding to *SiO* and Si_2O shows that films are of low density.

In contrast, Fig. 3 shows a deconvoluted Raman spectrum of a DLC film produced at α_t 30° and α_s 0° and the energy of *Xe* ions of 1.0 keV.

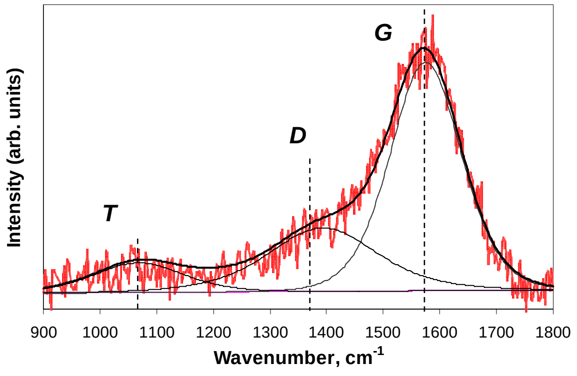

Fig. 3. UV Raman spectra of DLC films fabricated using the ion energy of 1.0 keV. HOPG target and the substrate were positioned at 30° and 0° (parallel) to the ion beam axis respectively.

The spectrum on Fig. 3 was decomposed by fitting a Pearson VII line function to all constituent peaks (Ref. 5). The best fit was obtained when using the Pearson width value *M*, of 5 for the *G* peak and 3 for the *D* and the *T* peaks. The spectra on Fig. 3 is dominated by the *G* peak located approximately at 1575 cm^{-1} and corresponding to stretching vibrations of aromatic rings and olefinic chains. The *D* peak is relatively small and positioned at 1390 cm^{-1}. The *T* peak contributions are seen and the peak is located at 1070 cm^{-1}. The relative intensity ratio of the *D* band to the *G* band, *I(D)/I(G)* was 0.28 and the *T* band to the *G* band, *I(T)/I(G)* was 0.13. Using the *I(T)/I(G)* ratio and the *T* peak position, cm^{-1} it is easy to distinguish DLCs with high sp^3 content from low sp^3. Using works of Ferrari and Robertson (Ref. 4), a *I(T)/I(G)* ratio below 0.2 indicates that sp^3 content is likely to be below 30 %, however sp^3 content of about 50 % corresponds to the *T* band position of 1070 cm^{-1}.

XPS C_{1s} spectra analysis was performed on all *a-C* and DLC samples in order to determine the sp^3/sp^2 ratio. The ration was obtained by decomposition of the C_{1s} core binding energy (BE) spectra onto two constituent functions corresponding to sp^2 and sp^3 carbon hybridization states. The deconvolution of DLC films fabricated at the ion energy of 1.0 keV and the target and the substrate angles of 30° and 0° is presented on Fig. 4.

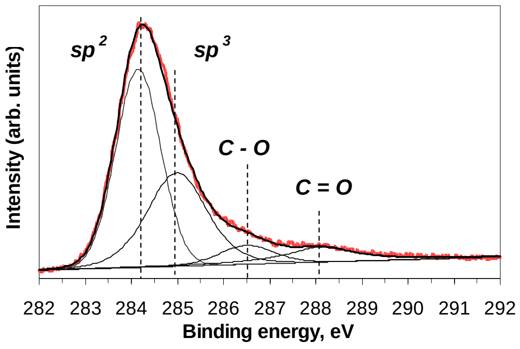

Fig. 4. The deconvolution of XPS C_{1s} spectra of DLC films fabricated using the ion energy of 1.0 keV and the target and the substrate angles to the ion beam axis were 30° and 0° respectively.

Due to the environmental oxidation two additional peaks were introduced into the fitting of the main C_{1s} spectra. These are, the single *C-O* bond at 286.5 eV and the double $C{=}O$ bond at 288 eV (Ref. 6). After subtracting the Shirley background the sp^2 and sp^3 peaks we fitted with Pearson VII function. Pearson's width value M, of 4 was used for carbon hybridized states and Gaussian lineshape was used for C-O and $C{=}O$ peaks. The comparative BE spectral functions of graphite (100% sp^2) and natural diamond (100% sp^3) were used to calculate the sp^3/sp^2 ratio based on the respective area ratios (Ref. 7). The sp^2 peak was found positioned at BE of 284.15 eV with FWHM_{sp2} of 1.15 eV and the sp^3 was at 285.0 eV with FWHM_{sp3} of 1.51 eV. The separation between the sp^2 and sp^3 constituents was 0.85. The sp^3/sp^2 ratio for DLC presented in Fig. 4 was found to be 0.41 ± 0.01. This is also within a value range for the sp^3 fraction for these DLC approximated by using the UV Raman results (Ref. 4). The summary of sp^3 content expressed in % ± 1 that was obtained using XPS C_{1s} analysis for all fabricated a-C and DLC films is presented in Table 3.

Table 3. The sp^3 content of fabricated a-C and DLC samples.

Ion beam energy, keV	Target and substrate to the ion beam axis sputtering angles, α_t/α_s° and sp^3 content, %					
	15/0	15/10	30/0	30/10	45/0	45/10
0.2			*SiC*			
0.4	*SiC*	*SiC*	<< 5	*SiC*	*SiC*	
0.6	<< 7	*SiC*	20	<< 7	<< 8	*SiC*
0.8	21	*SiC*	34	<< 7	24	*SiC*
1.0		<< 7	41	<< 8		<< 7

From Table 3 follows that at ion beam energies below 0.6 keV it was not possible to fabricate functional DLC films. At the substrate grazing angle of 10° to the ion beam axis there were no DLC films formed at any deposition energies independent to the target geometry. The obliteration of the forming DLC was caused by a secondary resputtering process. This is due to differentiation between sputter and nucleation energies, such as the energy of incident Xe ions is much higher than the threshold displacement energy of carbon atoms, while it is almost the same as or lesser than that of SiC atoms (Ref. 8).

4. Conclusion

DLC film can be synthesized on Si surface using a bi-modal ion beam sputtering, where a single ion beam is situated to sputter the graphite target at incident angles and the substrate is positioned parallel to the axis of the ion beam flux. At this arrangement the increase of incident ion energy promotes sp^3 bonding formation. However, positioning the substrate at grazing angles to the ion beam leads to a secondary resputtering process by the incoming ions and consequently no DLC film are formed.

Acknowledgements

The authors would like to thank J. Kavanagh, R. Helms and the staff of Laserdyne Pty Ltd for their welcome and the use of the laboratory. G. Hope of Griffith University for the use of UV Raman facilities and B. Wood of University of Queensland for the use of XPS facilities are gratefully acknowledged. This work has been supported by the Australian Research Council grant LP 0235814.

References

1. N. Savvides and B. Window, *J. Vacuum Sci. Tech. A* **3**, 2386-2390 (1985).
2. J. Bell, Z. Chen and A. Olofinjana, *Diamond Relat. Mater.* **10**, 2184-2189 (2001).
3. J. F. Ziegler, www.srim.org (1984-2006).
4. A. C. Ferrari and J. Robertson, *Phys. Rev. B: Condens. Matter Mater. Phys.* **64**, 075414 (2001).
5. M. Rybachuk and J. M. Bell, *Diamond Relat. Mater.* **15**, 977-981 (2006).
6. P. Merel, M. Tabbal, M. Chaker, S. Moisa and J. Margot, *Appl. Surf. Sci.* **136**, 105-110 (1998).
7. R. Haerle, E. Riedo, A. Pasquarello and A. Baldereschi, *Phys. Rev. B: Condens. Matter Mater. Phys.* **65**, 045101 (2002).
8. H. Heinisch, L. R. Greenwood, W. J. Weber and R. E. Williford, *J. Nucl. Mater.* **8**, 307 - 311 (2002).